Available online at www.sciencedirect.com

ScienceDirect

Energy Procedia 158 (2019) 2677–2682

Energy Procedia

www.elsevier.com/locate/procedia

The 10th International Conference on Applied Energy - ICAE2018

Daylighting simulation for external Venetian blinds based on HDR sky luminance monitoring with matrix algebraic approach

Yujie Wu[a], Jérôme Henri Kämpf[b], Jean-Louis Scartezzini[a]

[a]*Solar Energy and Building Physics Laboratory (LESO-PB), École polytechnique fédérale de Lausanne (EPFL), CH-1015, Lausanne, Switzerland*
[b]*Haute école d'ingénierie et d'architecture Fribourg, University of Applied Sciences Western Switzerland, CH-1700, Fribourg, Switzerland*

Abstract

An accurate daylighting simulation can potentially improve the quality of pre-planing buildings and regulating daylighting to achieve the goal of green buildings. However, standard sky models can hardly reproduce real skies in real-time for a specific location within its micro-climate. This paper investigates an embedded photometric device based on high dynamic range (HDR) sky luminance monitoring with high resolution mapping in simulating real-time horizontal work-plane illuminance distribution. To increase time efficiency in the iterative process for the illuminance calculation, a matrix algebraic approach was employed and adapted for the device. The photometric device was validated experimentally in a daylighting test module with external Venetian blinds at different tilt angle of slats. The results indicate the embedded photometric device based on monitored sky can improve accuracy in simulating real-time daylighting provision by over 3 times, with 15%~37% average error, compared with a common practice using the Perez all-weather model.

Keywords: Daylighting simulation; Embedded system; Five-phase method; Horizontal illuminance; Real-time

1. Introduction

Artificial lighting is a leading energy consuming entity in commercial buildings, which occupies around 15-30% in building energy consumption [1,2]. To reach the goal of high-performance green buildings, daylight, as a free source of illumination, has been exploited by designers and researchers over decades to increase the building energy efficiency. According to simulation and field-measurement results, studies have indicated optimal daylighting controls can potentially contribute to 30% to 70% saving in lighting electricity consumption [3]. Despite of its high luminous efficacy (70-130 lm/W), daylight can be converted into thermal energy after multiple reflections in buildings and can lead to a net increase in energy consumption when added cooling load exceeds saved lighting especially for over-glazed buildings [4]. Furthermore, the excessive penetration of daylight can also cause disturbing glare for occupants.

* Yujie Wu. Tel.: +41-21-693-3435 ; fax: +41-21-693-2722.
E-mail address: yujie.wu@epfl.ch

1876-6102
10.1016/j.egypro.2019.02.021

To overcome these challenging issues, daylighting simulation based on ray-tracing techniques is a common way to pre-plan buildings for designers and researchers. However, dynamic (real-time) regulation of daylighting has imposed increasingly high requirements on the accuracy and time resolution of simulation, since the sky conditions can change within minutes or even seconds due to the movement of clouds.

The daylighting simulation, as performed to date, is largely contingent on the sky luminance distribution models. However, sky models are commonly derived from averages of a range of sky types that can hardly reproduce the real sky at a specific location and time moment. The International Commission on Illumination (CIE) has defined 15 standard sky types, including the CIE clear, CIE overcast, and CIE intermediate sky [5]. Perez proposed a dynamic all-weather sky model based on direct and diffuse irradiance measurement [6], which is commonly used in the daylighting simulation. Nonetheless, studies have implied the pronounced sky luminance mismatch at regions close to horizon [7]. Furthermore, the Perez all-weather model, derived from sky luminance distribution monitored in Berkeley, CA, USA, does not necessarily represent skies at any part of the world. Fundamentally, according to the Shannon sampling theory, the spatial frequency of sampling input need to be at least two times more than that of the real sky to reproduce it without loss [8]. With only two inputs, the Perez all-weather model can have pronounced error in reproducing the real sky luminance distribution.

Although physically based rendering and ray-tracing techniques have been widely applied in lighting simulation of annual analysis and calculating daylighting metrics, the time consumption of computation is substantial for a single evaluation of a sky condition for merely one state of complex fenestration system (CFS). In 2006, Ward et al. proposed a matrix algebraic approach to discretize the daylighting computation with multiplication of pre-computed matrices (named three-phase method) which are generated based on ray-tracing techniques [9]. Although generation of the pre-computed matrix components is time consuming, the matrix algebraic approach reduces time in iterative calculation at a considerable scale for daylighting simulation, making the whole process time efficient for annual analysis or for operable CFS. However, noticeable error has been reported from validation studies due to the mismatch between the resolution ($10 - 15^{\circ}$) of bi-directional transmittance function (BTDF) [10] and the apex angle of the sun orb (0.53°) [11] when simulating CFS. McNeil et al. improved this technique by introducing additional matrices to compute the contribution from the sun orb separately with higher resolution in discretization (named five-phase method) [12].

In the light of the matrix algebraic approach for daylighting simulation, an embedded photometric device (EPD) [13,14] integrating the sky luminance monitoring based on high dynamic range (HDR) imaging techniques and real-time on-board daylighting simulation is to be evaluated in simulating the horizontal work-plane illuminance and to be validated with field measurement. The photometric device is able to map the luminance distribution of the sky vault and the ground with high resolution (1.23×10^6 subdivisions of the seen hemisphere), reproducing the real sky with increased accuracy than employing sky models. Its wide luminance detection range is able to detect the luminance of the sun orb, the sky, and landscape during daytime. In this paper, the five-phase matrix algebraic approach is assessed with adaptation for the EPD to simulate work-plane illuminance in a daylighting test module equipped with external Venetian blinds (EVB) with a sinusoid curved profile. The real-time simulation results are compared with those of a common practice employing the Perez all-weather sky model, contrasting the performance of the EPD.

2. Methodology and Experiments

A daylighting test module, with interior dimension $6.4 \times 2.9 \times 2.6\ m^3$, was selected for the 'in situ' experiments. The module was equipped with a south facing double-glazed unilateral façade, reaching a 0.62 window-to-wall ratio. An EVB was installed in front of the façade, with adjustable tilt angle of slats and retractable position, as shown in Figure 1 a). In this experiment, the position of the EVB was fully stretched and only different tilt angle of slats was investigated. The BTDF, characterizing the light transmitting behaviour of CFS, of the EVB with a sinusoid profile was computed by the 'genBSDF' program in RADIANCE software [15] based on ray-tracing techniques. To achieve precision in generating the BTDF, the slats of the EVB was modelled in RADIANCE with the identical geometry and with surface material property measured by a chromameter (MINOLTA CR-220) for its reflectance and by a gloss-meter (MINOLTA GM-060) for its specularity. Furthermore, the test module was modelled with precision in

the on-board RADIANCE program of the EPD. The dimension and relative position of each furniture were measured by a laser range finder, and the reflectance and specularity was monitored by the chromameter and the gloss-meter respectively for surface materials inside the daylighting module, including the ceiling, the wall, the floor, and surfaces of each furniture. To assess its real-time daylighting simulation, the EPD was positioned in front of the EVB, facing toward the sky vault, and the lens of the imaging system was aligned in the orthogonal plane of façade. The device monitored the luminance distribution of the sky vault (including the sun orb) and the ground based on HDR imaging techniques, mapped them into 1.23×10^6 directional subdivisions, and then simulated the horizontal work-plane (0.8 m height) illuminance at positions of 1 m, 2 m, 3 m, 3.9 m, and 4.7 m distance to the façade, employing the on-board RADIANCE software. As reference, an array of lux-meters was positioned at the identical positions inside the test module, as shown in Figure 1 b). The lux-meter array was connected to a data logger, recording illuminance values at corresponding positions simultaneously.

(a) The device positioned in front of the EVB

(b) Reference lux-meter array

Fig. 1. The experimental set-up for testing the embedded photometric device (EPD) in a daylighting test module

In simulating the horizontal illuminance distribution, the five-phase matrix algebraic approach is employed for the EPD to make iterative computation time efficient. The algebraic approach can be explained by Equation (1) [9,12]. The idea is to pre-compute matrices based on ray-tracing techniques (time consuming) relating the monitored sky luminance distribution to the target work-plane illuminance. The matrix multiplication (time efficient) of **VTDs** in Equation (1) computes the work-plane illuminance contributing from a coarsely discretized sky, which is the same as the three-phase matrix algebraic approach [9]. The matrix multiplication of $\mathbf{C}_{ds}\mathbf{s}_{sun}$ extracts the sun orb from the sky at a finer resolution and calculates the daylighting contribution from the sun with an improved accuracy. To exclude the overlapping computation of the solar component, the daylighting contribution from the sun orb ($\mathbf{V}_d\mathbf{TD}_d\mathbf{s}_{ds}$) at coarse resolution need to be subtracted from the result of **VTDs**. Since the original five-phase matrix algebraic approach was designed for sky models, the approach need to be adapted in the case of the EPD based on HDR sky luminance monitoring. Instead of subdividing the sky vault only, the hemisphere including both the sky vault and the ground that the façade is facing toward is subdivided according to the Tregenza-based sky division scheme [16], sub-sampling of the luminance map (resolution 1.2×10^6) into 2306 patches for $\mathbf{s}$ and $\mathbf{s}_{ds}$, because only the south-facing hemisphere of the sky vault and the ground contribute daylighting in the module. The solar component is extracted from the luminance map of the sky with monitored luminance value of the sun orb. The sun position is discretized into one of 5176 locations according to the Tregenza-based sky division scheme, and is approximated to the closest discrete location, with maximal bias 1.5°. The BTDF is generated by the 'genBSDF' program with Klems angular basis, with 145×145 incident and exit directions, for $\mathbf{T}$ in Equation (1) to calculate the work-plane illuminance contributing from the sky vector. For the solar contribution, the geometry of the EVB is employed to compute the solar coefficient matrix $\mathbf{C}_{ds}$ with higher resolution in calculating the contribution from the sun orb in work-plane illuminance (lx).

$$\mathbf{i}_{5ph} = \mathbf{VTDs} - \mathbf{V}_d\mathbf{TD}_d\mathbf{s}_{ds} + \mathbf{C}_{ds}\mathbf{s}_{sun} \tag{1}$$

- $\mathbf{i}_{5ph}$ is a vector containing the computed work-plane illuminance at corresponding position in the test module
- $\mathbf{s}$ is the sky vector, containing the luminance distribution of the subdivided sky as input
- $\mathbf{s}_{ds}$ is the direct sky vector, a sparse vector containing only the luminance of the coarse resolution solar patch

- $\mathbf{s}_{sun}$ is the direct sun vector, a sparse vector containing only the luminance of the fine resolution solar patch
- $\mathbf{D}$ is the daylight matrix, relating sky luminance distribution to incident directions on the front EVB plane
- $\mathbf{D}_d$ is the direct daylight matrix, similar to $\mathbf{D}$ but excluding interreflections from the ground or surrounding objects
- $\mathbf{T}$ is the transmission matrix (BTDF), relating light flux transfer from incident directions on the front EVB plane to exit directions on the interior side of the window façade
- $\mathbf{V}$ is the view matrix, relating the contribution from each exit direction from the window (interior) to the work-plane illuminance at corresponding positions
- $\mathbf{V}_d$ is the direct view matrix, similar to $\mathbf{V}$ but only relating the solar component (coarse resolution) excluding interreflection in the module
- $\mathbf{C}_{ds}$ is the solar coefficient matrix, relating the contribution from the solar component (fine resolution) to the work-plane illuminance at corresponding positions

In the experimental validation, both the EPD and the reference lux-meter array were synchronized every 15 min to simulate and monitor horizontal work-plane illuminance respectively. For contrasting the performance, the direct normal and diffuse horizontal irradiance was monitored at the rooftop of the daylighting test module simultaneously without shadowing and was used as input for the Perez all-weather sky model to simulate the work-plane illuminance at the identical positions, employing the original five-phase matrix algebraic approach.

3. Experimental results

The daylighting experiment was conducted under a partly cloudy sky, when the contrast between different parts of the sky was substantial. The EVB was fully stretched, covering the façade, and its slat tilt angle was fixed at 32° to the vertical plane. The horizontal work-plane illuminance was simulated and monitored every 15 min from 9:00 to 18:00 for the daylighting test module. Each iteration of matrix multiplication can be accomplished within 10 s on the embedded platform, compared with 15-20 min by using the ray-tracing algorithm reaching a similar quality of simulation. The results simulated by using the EPD based on HDR sky luminance monitoring is illustrated in Figure 2 a), where the five stacked green lines represent the illuminance simulated at positions of 1 m, 2 m, 3 m, 3.9 m, and 4.7 m to the façade respectively. The stacked grey lines denote the monitored illuminance values by using the lux-meter array. For comparison, the work-plane illuminance is also simulated employing a common practice using the Perez all-weather model, as shown in Figure 2 b) with stacked green lines. Although both are based on the five-phase matrix algebraic method, the simulation by using the EPD based on HDR sky luminance monitoring shows higher concordance with the reference value than using the Perez sky model. The relative error is illustrated in Figure 3 for the two different sky reproducing methods respectively. According to the error bar, the simulated illuminance by using the EPD based on sky luminance monitoring, of which the average relative errors for the 5 positions are 16.5%, 15.0%, 16.1%, 15.8%, and 17.8% respectively, reduces the error in a pronounced scale than the common practice using the Perez all-weather model, of which the average errors are 341%, 319%, 266 %, 244 %, and 240% respectively.

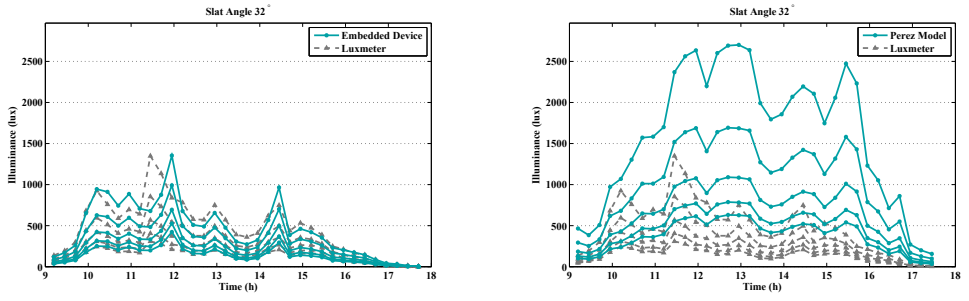

(a) Embedded device (b) Perez all-weather model

Fig. 2. Simulated horizontal work-plane illuminance by using the two approaches to reproduce the sky (32° tilt angle)

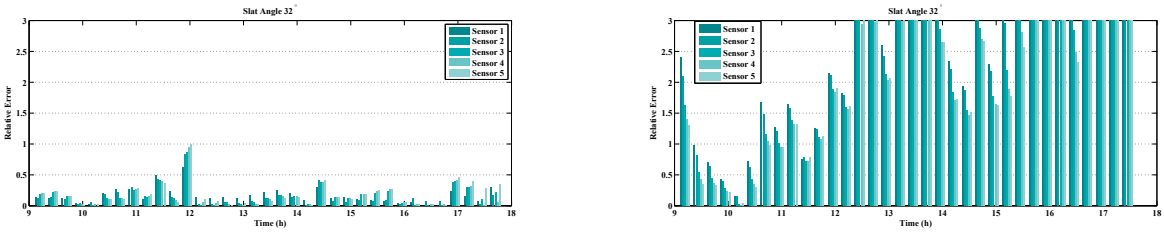

(a) Embedded device (b) Perez all-weather model

Fig. 3. Relative error in the simulated horizontal work-plane illuminance by using the two approaches (32° tilt angle)

For slats fixed at tilt angle 72° to the vertical plane (larger opening of EVB), the experiment was conducted in a similar way under a partly cloudy sky. The simulated horizontal work-plane illuminance is illustrated in Figure 4 represented by stacked green lines for the EPD based on HDR sky luminance monitoring and for a common practice employing the Perez all-weather model respectively. According to the mismatch, the EPD based on monitored sky outperforms the common practice employing the Perez all-weather model in simulating work-plane illuminance distribution. In particular, the Perez sky model contributed to pronounced error in the early morning and late afternoon in dim environments, when the sky was covered with dense clouds and had a peaky luminance distribution. The relative error of work-plane illuminance for the two approaches reproducing the sky is illustrated in Figure 5. The average relative error at the 5 positions by using the EPD is 36.3%, 35.6%, 34.9%, 15.5%, and 16.7% respectively, while that employing the Perez all-weather model is 203%, 150%, 124%, 111%, and 120% respectively. The spikes of error at noon and the relative higher error of the front three virtual sensors for the EPD is possibly due to the bias of solar position from discretization, which can potentially be improved by increasing its resolution.

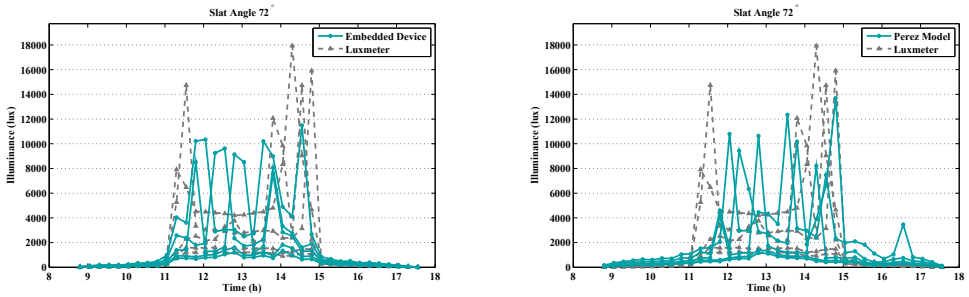

(a) Embedded device (b) Perez all-weather model

Fig. 4. Simulated horizontal work-plane illuminance by using the two approaches to reproduce the sky (72° tilt angle)

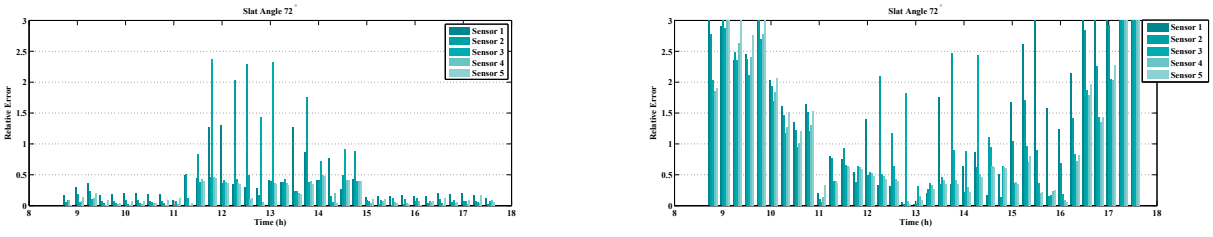

(a) Embedded device (b) Perez all-weather model

Fig. 5. Relative error in the simulated horizontal work-plane illuminance by using the two approaches (72° tilt angle)

4. Conclusion

The mismatch between the real sky and sky models can contribute to pronounced error in transient daylighting simulation due to the fact that sky models cannot reproduce skies accurately in real-time, especially when the sky has a peaky luminance distribution. In this paper, an embedded photometric device (EPD) based on HDR sky luminance monitoring with high resolution was validated experimentally in simulating the horizontal work-plane illuminance in a daylighting test module equipped with an EVB with sinusoidal profile. The five-phase algebraic approach was adapted for the EPD to simulate the work-plane illuminance, reducing the iteration time to 10 s from over 15 min employing ray-tracing approach, increasing the time-resolution in simulating real-time daylighting provision. Comparing with a common practice employing the Perez all-weather model, the EPD based on monitored sky with high resolution mapping shows an improved accuracy (over 3 times) in simulating work-plane illuminance at different tilt angles of slats of the EVB, with 15% $\sim$ 37% average error. The simulation results indicate its improved accuracy in reproducing the real sky in real-time than employing sky models. The EPD with high accuracy and time-resolution in simulating daylighting provision would show its merits in daylighting analysis and real-time daylighting control for high-performance buildings, which will be further studied in the future work.

ACKNOWLEDGEMENT

The authors would like to thank the Commission for Technology and Innovation of Switzerland for funding Swiss Competence Center for Energy Research (SCCER), Future Energy Efficiency Buildings and District (FEEB&D).

References

[1] M. Krarti, *Energy audit of building systems: an engineering approach*. CRC press, 2016.
[2] J. C. Lam, D. H. Li, and S. Cheung, "An analysis of electricity end-use in air-conditioned office buildings in hong kong," *Building and Environment*, vol. 38, no. 3, pp. 493–498, 2003.
[3] L. Doulos, A. Tsangrassoulis, and F. Topalis, "Quantifying energy savings in daylight responsive systems: The role of dimming electronic ballasts," *Energy and Buildings*, vol. 40, no. 1, pp. 36–50, 2008.
[4] J. Mardaljevic, L. Heschong, and E. Lee, "Daylight metrics and energy savings," *Lighting Research & Technology*, vol. 41, no. 3, pp. 261–283, 2009.
[5] C. Standard, "Spatial distribution of daylight-cie standard general sky," *CIE S*, vol. 11, 2003.
[6] R. Perez, R. Seals, and J. Michalsky, "All-weather model for sky luminance distributionpreliminary configuration and validation," *Solar energy*, vol. 50, no. 3, pp. 235–245, 1993.
[7] M. B. Piderit, C. Cauwerts, and M. Diaz, "Definition of the cie standard skies and application of high dynamic range imaging technique to characterize the spatial distribution of daylight in chile," *Revista de la Construcción*, vol. 13, no. 2, 2014.
[8] C. E. Shannon, "Communication in the presence of noise," *Proceedings of the IRE*, vol. 37, no. 1, pp. 10–21, 1949.
[9] G. Ward, R. Mistrick, E. S. Lee, A. McNeil, and J. Jonsson, "Simulating the daylight performance of complex fenestration systems using bidirectional scattering distribution functions within radiance," *Leukos*, vol. 7, no. 4, pp. 241–261, 2011.
[10] F. Bartell, E. Dereniak, and W. Wolfe, "The theory and measurement of bidirectional reflectance distribution function (brdf) and bidirectional transmittance distribution function (btdf)," in *Radiation scattering in optical systems*, vol. 257, pp. 154–161, International Society for Optics and Photonics, 1981.
[11] E. S. Lee, D. Geisler-Moroder, and G. Ward, "Modeling the direct sun component in buildings using matrix algebraic approaches: Methods and validation," *Solar Energy*, vol. 160, pp. 380–395, 2018.
[12] A. McNeil, "The five-phase method for simulating complex fenestration with radiance," *Lawrence Berkeley National Laboratory, Berkeley, CA, USA*, 2013.
[13] Y. Wu, J. H. Këmpf, and J.-L. Scartezzini, "An embedded system for quasi real-time lighting computation based on sky monitoring," in *15th IBPSA Building Simulation 2017*, (San Francisco, USA), August 2017.
[14] Y. Wu, J. H. Këmpf, and J.-L. Scartezzini, "Characterization of a quasi-real-time lighting computing system based on hdr imaging," *Energy Procedia*, vol. 122, pp. 649–654, 2017.
[15] G. W. Larson and R. Shakespeare, *Rendering with Radiance: the art and science of lighting visualization*. Booksurge Llc, 2004.
[16] D. Bourgeois, C. F. Reinhart, and G. Ward, "Standard daylight coefficient model for dynamic daylighting simulations," *Building Research & Information*, vol. 36, no. 1, pp. 68–82, 2008.